



CHORUS

This is the accepted manuscript made available via CHORUS. The article has been published as:

Observation of the Kondo effect in a quadruple quantum dot

Runan Shang, Hai-Ou Li, Gang Cao, Guodong Yu, Ming Xiao, Tao Tu, Guang-Can Guo, Hongwen Jiang, A. M. Chang, and Guo-Ping Guo

Phys. Rev. B **91**, 245102 — Published 2 June 2015

DOI: [10.1103/PhysRevB.91.245102](https://doi.org/10.1103/PhysRevB.91.245102)

Observation of the Kondo Effect in a Quadruple Quantum Dot

*Runan Shang,^{1,2} Hai-Ou Li^{1,2}, Gang Cao^{1,2}, Guodong Yu^{1,2}, Ming Xiao,^{1,2} Tao Tu^{1,2},
Guang-Can Guo^{1,2}, Hongwen Jiang³, A.M.Chang^{4*}, and Guo-Ping Guo^{1,2}†*

1 Key Laboratory of Quantum Information, University of Science and Technology of China, Chinese Academy of Sciences, Hefei 230026, P.R.China;

2 Synergetic Innovation Center of Quantum Information & Quantum Physics, University of Science and Technology of China, Hefei, Anhui 230026, P.R.China

3 Department of Physics and Astronomy, University of California at Los Angeles, California 90095, USA.

4 Department of Physics, Duke University, Durham, NC 27708-0305, USA

ABSTRACT: We investigate the Kondo effect in a quadruple quantum dot device of coupled-double quantum dots (DQDs), which simultaneously contains intra-DQDs and inter-DQDs coupling. A variety of novel behaviors are observed. The differential conductance dI/dV is measured in the upper DQDs as a function of source drain bias. It is found to exhibit multiple peaks, including a zero-bias peak, where the number of peaks exceeds five. Alternatively, tuning the lower DQDs yielded regions of four peaks. In addition, a Kondo-effect switcher is demonstrated, using the lower DQDs as the controller.

* Corresponding author: yingshe@phy.duke.edu

† Corresponding author: gpguo@ustc.edu.cn

In the past few years, substantial progress on manipulating heterostructure quantum dot (QD)¹⁻¹⁰ has made it possible to tune system parameters very precisely. This provides a powerful tool for studying the Kondo effect which is an intrinsic many-body phenomenon due to the interplay of localized magnetic impurity and itinerant conduction electrons. Many experimental and theoretical works have been done and provide firm understanding for the Kondo effect on single quantum dot^{1,20}. On double quantum dots (DQDs) the physics become more diverse. A variety of quantum phenomena are found, such as a transition between different quantum states^{5,6}. On the basis of a relatively clear picture in the double dots system, some further study on the triple^{11,12} and quadruple dots^{13,19} in theory has been done. Several interesting physics, such as the Berezinskii-Kosterlitz-Thouless phase transition²⁶ or the existing of charge Kondo state, may be realized on these multiple dot systems. However, experiments that could pin them down are still lacking, partially due to the increasing difficulties in much more subtle electrical tuning on the multiple dots system.

In this Letter, we study a quadruple QDs system which consists of two sets of DQDs and three types of interaction: 1. the Kondo coupling between the dots and their corresponding reservoir; 2. the Heisenberg coupling between the two dots within each DQDs; 3. the Ising coupling between the two sets of DQDs. The situations with only Heisenberg^{10,14,15} or Ising coupling^{16,17} have been studied in DQDs but experimental study with both couplings has never been reported to the best of our knowledge. In the following, we report our observations in such a quadruple QDs system.

Our sample is fabricated on the *GaAs/Al_{0.3}Ga_{0.7}As* heterostructure which contains a two-dimensional electron gas (2DEG) lying 100nm below the wafer surface with electron density $2.3 \times 10^{11} \text{ cm}^{-2}$ and mobility $1.5 \times 10^5 \text{ cm}^2/\text{V} \cdot \text{s}$. The sample is placed in a dilution refrigerator with base temperature of 40mK.

Fig.1 (d) shows our device structure. Gates 1-5 define a typical series-coupled DQDs structure (upper set of DQDs, UDQDs). The lower set of DQDs (LDQDs) is formed using the gates 6-10. These two sets of DQDs are divided by a pair of horizontal gates 11 and 12 and capacitively coupled to each other. The differential conductance $G=dI/dV$ through the UDQDs and LDQDs is measured using the standard lock-in technique. When the upper and lower DQDs work independently, the negative voltage applied on gates 11 and 12 creates a high enough barrier for the electrons and the probability for them to tunnel through is negligible. The charge state of a set of DQDs can be represented as $(N,M)_i$ which means there are N electrons in the left dot and M electrons in the right dot while $i=U,D$ distinguishes the upper or lower DQDs. Fig.1 (a) and Fig.1 (b) illustrate the stability diagram of each DQDs and the states.

Parameters characterizing our system can be extracted from the honey-comb diagrams²¹ and are essential for the ensuing discussion. For the UDQDs, the left/right dot charging energies U_{UL}/U_{UR} have almost the same value of 340GHz. The tunneling rate Γ_{UL} from the upper left dot to the reservoir, as estimated from the full width at half maximum of Coulomb blockade peak, is about 18GHz. For Γ_{UR} , Γ_{DR}

and Γ_{DL} it is difficult to determine them from obscure Coulomb peak. The capacitive coupling between the left and right dot E_{Um} is about 16GHz. For the lower DQDs, U_{DL} is about 590GHz and U_{DR} is about 530GHz. The coupling between the left and right dots of LDQDs is about 15GHz. The interactions value between the two sets of DQDs is about 8GHz from the line shift¹⁸ as in Fig. 1 (c). The intra-dot tunneling coupling of the UDQDs measured by the photon-assisted-tunneling method²² is about 7GHz.

In this work, the upper and lower DQDs are capacitively-coupled throughout, while we tune the intra-dot tunneling coupling for the upper and/or lower DQDs. Carefully tuning every gate, the most notable feature of the Kondo effect, a zero bias peak (ZBP), is observed in the UDQDs [in Fig.2 (a)]. Here the gate voltages are $V_{1-12} = -0.63V, -0.7V, -0.65V, -0.7V, -0.945V, -0.81V, -0.4V, -0.55V, -0.4V, -0.84V, -0.8V, -0.8V$ (V_1 stands for voltage on gate1, and so on). Here, Both UDQDs and LDQDs are formed. Upon increasing the base temperature from 50mK to 800mK, the ZBP height undergoes a monotonous decreasing from the highest value $0.082e^2/h$ as shown in Fig.2 (b) (a constant value is subtracted as background). This enables us to deduce the Kondo temperature here is about between 800-900mK.

To establish that the ZBP is due to the Kondo effect, we change slightly V_3 while keeping the other voltages fixed ($V_6 = -0.774V, V_{10} = -0.885V$). As a consequence, the intra-dot coupling in UDQDs is modulated, which offers us an opportunity to observe the quantum state transition from atomic Kondo state to coherent bonding Kondo, where the tunneling coupling induces a coherent superposition of the individual Kondo state between QDs, or anti-ferromagnetic state, where the anti-ferromagnetic coupling induce the two impurities moment into a singlet state and the net moment is zero^{5,6}. Fig.2 (a) shows the picture with V_3 changing from $-0.651V$ to $-0.645V$, where a less negative voltage corresponds to a larger intra-dot coupling. We found the result that the splitting between single peak and double peaks occurs at about $V_3 = -0.648V$. When V_3 is adjusted along the positive direction the double splitting peaks become more and more asymmetric, which may arise as the electrons wavefunction in UDQDs becomes asymmetric with the sizable increase in the gate voltage.

For simplicity, in UDQDs, we assume Γ equals to Γ_{UL} and intra-dot coupling t equals to $E_{Um} = 16GHz$. The state transition here can be determined as atomic-Kondo state to coherent bonding Kondo state^{24,25} considering the fact t/Γ is close to 1 but $j = 4t^2T_K/U_{UL}$ is far away from the critical value of 2.5. The change of intra-dot coupling around the transition is too small to be checked for the splitting process spans less than 1mV.

It is worth pointing out that the presence of the ZBP, along with the occurrence of at least two additional peaks on each side when we tune the double horizontal gate V_{11} and V_{12} [indicated by red dashed lines in Fig.2 (c) inset], has not been found in previous studies. The temperature dependence is shown in Fig.2 (c) by a series of dI/dV curves, corresponding to the white line in Fig.2 (c) inset, from 50mK (bottom) to 250mK (top). Here, it is important to rule out spurious effects, such as from an interference path between the exit of the DQDs and an accidental defect in the 2DEG, as the cause of these smaller oscillations. Such a path can act as a Fabry-Perot

interferometer, and in principle, give rise to a modulation in the transmission probability as the energy (bias voltage) is varied. We can estimate a path length of $L \sim 4 \mu m$ from the oscillation spacing of $100 \mu eV$ and the density of $2.3 \times 10^{11} cm^{-2}$. The transport mean free path is $L_m \sim 1.19 \mu m$. However, here, it is the small angle scattering length that matters, which is considerably shorter. Previous studies indicates a rough factor of 4 reduction²³, or $L_m \sim 0.3 \mu m$. To have interference requires both the forward and reflected path, giving a total distance of $2L \sim 8 \mu m$. It is inconceivable that the interference features will survive, with $N = 8 \mu m / 0.3 \mu m \sim 26.7$ scattering events, leaving probability of the direct path surviving as $e^{-26.7} \sim 10^{-11}$. So we can attribute these features to the DQDs system.

Existence of the other set of DQDs may result in new phenomena that are beyond what can be observed in a single set of DQDs only. Keeping the UDQDs voltages ($V_{1-5,11,12} = -0.63V, -0.7V, -0.65V, -0.7V, -0.945V, -0.7995V, -0.7995V$), we sweep along the line from ($V_6 = -0.855, V_{10} = -0.807V$) to ($V_6 = -0.752V, V_{10} = -0.919V$) while measuring the dI/dV of the UDQDs. The result of this measurement is presented in Fig.3 (a). Decreasing V_{10} from $-0.807V$, a ZBP is observed and the peak height grows up to about $0.08e^2/h$ at $V_{10} = -0.85V$. At the same time, the other double peaks (indicated by red dashed lines) emerge on the opposite side from $V_{10} = -0.825V$ and grow closer when V_{10} becomes more negative. This scenario is very similar to what was found by Okazaki et. al.⁷, who studied the orbital degree of freedom in the Kondo effect for a parallel-coupled DQDs system.

Keeping our sweeping process, the ZBP splitting occurs as V_{10} reaches about $-0.85V$. We speculate this as indicative of a transition from a Kondo regime to a bonding-singlet of individual Kondo states, similar to what was observed when tuning V_3 as in Fig.2 (a). The height of the leftmost peak is enhanced and becomes parallel to the middle double peaks while the rightmost peak does not show the same enhancement behavior but it could still be distinguished in Fig.3 (a). At $V_{10} = -0.866V$, there is a shift (indicated by black dashed line) occurring when charge number transition happens in LDQDs. Neglecting this shift, four peaks (indicated by red dashed lines) are seen to appear following a splitting process, although the rightmost one is relatively obscure.

To determine whether the peaks and splitting arise from the interaction between the UDQDs and LDQDs or from the capacitive coupling between the upper and lower gates, we remove the LDQDs and repeat our experiment. V_7 and V_9 are set to 0 from $-0.4V$ and others are fixed. No quantum dot forms as the current through the source to drain of original LDQDs structure is several hundreds of pA. The UDQDs charging diagram changed minimally by directly comparing the diagram with $V_9 = -0.4V$ and $V_9 = 0$ (not shown here), where only a $-10mV$ shift in V_5 is found.

We label the two cases as I (with LDQDs forming) and II (without the LDQDs forming). Under the same charging state $(N, M)_U$, we observed the evolution of the Kondo peaks when V_6 and V_{10} are changed simultaneously as in case I from ($V_6 = -0.73, V_{10} = -0.86V$) to ($V_6 = -0.55V, V_{10} = -1.04V$). The result of dI/dV is presented in Fig.3 (b). The ZBP, which spans the entire diagram, is illustrated by a black dashed line. Other two white dashed lines indicate the converging double bumps. There are

some obvious differences with case I: Firstly, by removing the LDQDs, there is no longer any regime of a split-peaks at zero bias, nor the four-peaks feature [as Fig.3 (e)], but instead, all traces exhibit a ZBP, which spans the entire V_{10} range, even though V_6 and V_{10} were varied over a much wider range than in case I. Moreover, the converging peaks collapse from higher peak in case I to lower bump in case II, which suggests the decreasing of Kondo temperature. When V_{10} is more negative than -0.93V , the converging double peaks vanished. Secondly, comparing the height of ZBP in the range of three peaks existence (ZBP with two converging peaks), we find that the ZBP reaches $0.086e^2/h$ [see Fig.3 (d), background subtracted] in case I while the ZBP is about $0.052e^2/h$ in case II [see Fig.3 (c), background subtracted] and remains almost unchanged with V_{10} . The weakening of the Kondo effect cannot be explained as coming from the modulation of the lower plunger gates because the peak would be higher rather than lower if it is only influenced by the capacitive coupling between the gates. These suggest the possibility that the ZBP enhancement in case I could be due to the presence of LDQDs.

Finally, we discuss the shift in Fig.3 (a) (LDQDs charge transition). The charge repopulation between $(N+1, M)_D$ and $(N, M+1)_D$ will induce a shift of the entire diagram of the UDQDs according to the capacitive coupling between the two sets of DQDs. Two curves extracted from Fig.3 (a) at $V_{10}=-0.851\text{V}$ and $V_{10}=-0.87\text{V}$ are shown in Fig.4 (a). They are nearly identical except the rightmost background. This finding may be interpreted as follows: when sweeping along a chosen control line in the LDQDs, a given point in the UDQDs experiences a corresponding shift in the value of its voltage parameters. When a state transitions from $(N+1, M)_D$ to $(N, M+1)_D$ occurs in the control line, the fixed point would be shifted back to a former set of the parameter values. That provides us a chance to switch Kondo state with a control qubit. We slightly tune the double horizontal gates from $V_{11}=V_{12}=-0.7995\text{V}$ to $V_{11}=V_{12}=-0.8003\text{V}$, keeping other gates voltages unchanged, then we scan V_{10} and draw the data into Fig.4 (b), causing a transition to a higher ZBP ($0.0562e^2/h$) compared with a rather weaker one ($0.0362e^2/h$) at the opposite contiguous area of the shift (indicated by the white dashed line and arrows). We are confident that we will be able to realize an on/off Kondo switcher, once a more refined gate operation is implemented into this quadruple dots system.

These findings illustrate the many exciting phenomena we uncovered, which have not been observed before; however, we are not aware of any theoretical work that provides a satisfactory explanation for them.

In summary, the Kondo effect was observed in an electrically-coupled quadruple dots system. Several unusual features were found: a ZBP with at least two additional peaks on each side of bias voltage has not been previously reported. Moreover, a splitting indicating a transition from an atomic-like Kondo to a coherent single Kondo state appears in the UDQDs when we tuned the LDQDs, giving rise to a four peaks feature in the dI/dV . By removing the LDQDs while maintain the gating voltage on the pincher gates controlling intra-dot coupling, we are able to demonstrate that the transition phenomenon arises from inter-dot coupling. To further investigate these novel behaviors will require the application of an in-plane magnetic field, which will

be helpful in establishing the physical mechanism responsible for the novel behaviors.

Acknowledgements:

This work was supported by the National Fundamental Research Programme (Grant No. 2011CBA00200), National Natural Science Foundation (Grant Nos. 11222438, 10934006, 11274294, 11074243, 11174267, 91121014 and 11474270), NSF-DMR and the Academia Sinica, Taipei.

References

- [1] M. Grobis, I. G. Rau, R. M. Potok, and D. Goldhaber-Gordon, arXiv:cond-mat/0611480
- [2] D. Goldhaber-Gordon, Hadas Shtrikman, D. Mahalu, David Abusch-Magder, U. Meirav, and M. A. Kastner *Nature* 391,156 (1998)
- [3] Sara M. Cronenwett, Tjerk H. Oosterkamp, and Leo P. Kouwenhoven *Science* 281,540 (1998)
- [4] A. Kogan, G. Granger, M. A. Kastner, D. Goldhaber-Gordon, and H. Shtrikman *Phys.Rev.B* 67,113309 (2003)
- [5] H. Jeong, A. M. Chang, and M. R. Melloch *Science* 293,2221 (2001)
- [6] J. C. Chen, A.M. Chang, and M. R. Melloch *Phys.Rev.Lett* 92,176801 (2004)
- [7] Yuma Okazaki, Satoshi Sasaki, and Koji Muraki *Phys. Rev. B* 84, 161305 (2011)
- [8] N. J. Craig, J. M. Taylor, E. A. Lester, C. M. Marcus, M. P. Hanson, and A. C. Gossard *Science* 304,565 (2004)
- [9] R. M. Potok, I. G. Rau, Hadas Shtrikman, Yuval Oreg, and D. Goldhaber-Gordon *Nature* 446,167 (2007)
- [10] A. M. Chang, and J. C. Chen *Rep.Prog.Phys.* 72,096501 (2009)
- [11] P. P. Baruselli, R. Requist, M. Fabrizio, and E. Tosatti *Phys.Rev.Lett* 111,047201(2013)
- [12] Rosa L'opez, Tomaz Rejec, Jan Martinek, and Rok Zitko *Phys. Rev. B* 87,035135(2013)
- [13] Dong E. Liu, Shailesh Chandrasekharan, and Harold U. Baranger *Phys.Rev.Lett.* 105,256801 (2010)
- [14] I. Affleck, A.W.W. Ludwig, and B. A. Jones, *Phys. Rev. B* 52, 9528 (1995)
- [15] G. Zaránd, C.-H. Chung, P. Simon, and M. Vojta, *Phys.Rev. Lett.* 97, 166802 (2006)
- [16] M. Garst, S. Kehrein, T. Pruschke, A. Rosch, and M. Vojta, *Phys. Rev. B* 69, 214413 (2004).
- [17] M. R. Galpin, D. E. Logan, and H. R. Krishnamurthy, *Phys. Rev. Lett.* 94, 186406 (2005);
- [18] K. D. Petersson, C. G. Smith, D. Anderson, P. Atkinson, G. A. C. Jones, and D. A. Ritchie *Phys.Rev.Lett.* 103,016805 (2009)
- [19] Gou Shinkai, Toshiaki Hayashi, Takeshi Ota, and Toshimasa Fujisawa *Phys.Rev.Lett.* 103,056802 (2009)
- [20] M. D. Shulman, O. E. Dial, S. P. Harvey, H. Bluhm, V. Umansky, and A. Yacoby *Science* 336,202 (2012)
- [21] W. G. van der Wiel, S. De Franceschi, J. M. Elzerman, T. Fujisawa, S. Tarucha, and L. P. Kouwenhoven *Rev.Mod.Phys.* 75,1 (2003)

- [22] Runan Shang, Haiou Li, Gang Cao, Ming Xiao, Tao Tu, Guang-Can Guo, Hong-Wen Jiang, and Guo-Ping Guo *Appl. Phys. Lett.* 103, 162109 (2013);
- [23] A.M. Chang, H.U. Baranger, L.N. Pfeiffer, and K.W. West, *Phys.Rev.Lett* 73, 2111 (1994)
- [24] Ramón Aguado, and David C. Langreth *Phys. Rev. Lett.* 85 1946 (2000)
- [25] B. A. Jones, and C. M. Varma *Phys. Rev. Lett.* 58 843 (1987)
- [26] Walter Hofstetter, and Herbert Schoeller *Phys.Rev.Lett.* 88,016803 (2001)

Figure Captions:

Figure1 (a) The figure shows a honey-comb diagram with charge states $(N,M)_U$, $(N+1,M)_U$, $(N,M+1)_U$ and $(N+1,M+1)_U$ (b) The figure shows charge states $(N, M)_D$, $(N+1, M)_D$, $(N, M+1)_D$ and $(N+1, M+1)_D$ (c) The shift at $V_1=-0.785V$ shows the coupling strength as 8GHz between upper DQDs and lower DQDs by sweeping across the charge transition from $(N,M)_D$ to $(N+1,M)_D$. (d) The SEM picture of the quadruple dots system. The black dots 'us' and 'ud' present the source and drain of upper DQDs while 'ds' and 'dd' present the source and drain of lower DQDs.

Figure2 (a) The figure shows the dI/dV while changing the V_3 from $-0.651V$ to $-0.645V$. A splitting (indicated by white dashed lines) occurs at about $V_3=-0.648V$. ($V_6=-0.774V$, $V_{10}=-0.885V$) (b) The curve illustrates the dependence of ZBP with base temperature (background extracted). (c) Successive dI/dV curves ($V_6=-0.81V$, $V_{10}=-0.84V$, temperature at 50mK, 60mK, 70mK, 80mK, 100mK, 150mK, 200mK and 250mK from bottom to top curve). They are offset by $0.05e^2/h$ and drawn together. The curve is extracted from the white line in inset, which draws dI/dV dependence on V_{11} (V_{12} is always equal to V_{11}). Five peaks are indicated by red dashed lines.

Figure3 (a) The figure draws the dI/dV through UDQDs while sweeping from ($V_6=-0.855V$, $V_{10}=-0.807V$) to ($V_6=-0.752V$, $V_{10}=-0.919V$) and the Kondo peaks are indicated by red dashed line. ZBP with other two converging peaks appear from $V_{10}=-0.825V$ to $V_{10}=-0.85V$. Then ZBP splits to double peak and a new feature of four Kondo peaks are formed (case I). At $V_{10}=-0.866V$, there is a shift (indicated by black dashed line) that occurs corresponding to the charge number transition of LDQDs. (b) The plunger gates V_7 and V_9 are set from $-0.4V$ to 0 (case II). dI/dV is read out while sweeping from ($V_6=-0.73V$ $V_{10}=-0.86V$) to ($V_6=-0.55V$ $V_{10}=-1.04V$) (The shift at $V_{10}=-0.875V$ results from an occasional random shift which should be omitted). The converging double peaks (by white dashed line) have become a lower bump but keep the converging behavior from $V_{10}=-0.86V$ to $V_{10}=-0.93V$ as well. They finally disappear when V_{10} is more negative. (c) This curve is extracted from the red dashed line ($V_{10}=-0.87V$) in Fig. 3 (b). (d) and (e) The curves are from the dashed yellow lines ($V_{10}=-0.835V$, $V_{10}=-0.895V$) in Fig. 3 (a). In (c), height of ZBP obviously decreases to $0.052e^2/h$ and stays almost unchanged during the whole sweeping process while height of ZBP is $0.086e^2/h$ in (d). There is no splitting appearing in (b). That is entirely different from (e) which illustrates a four-peaks feature clearly.

Figure4 (a) Two dI/dV curves extracted from Fig.3 (a) with $V_{10}=-0.851V$ and $V_{10}=-0.87V$ are compared, they are almost identical except the right background. (b) Changing the V_{11} and V_{12} from $-0.7995V$ to $-0.8003V$ and scan the V_{10} , the ZBP experiences a strong step at about $V_{10}=-0.866V$, indicated by white dashed line and arrows. A Kondo effect switcher might be realized using the LDQDs as a controller.

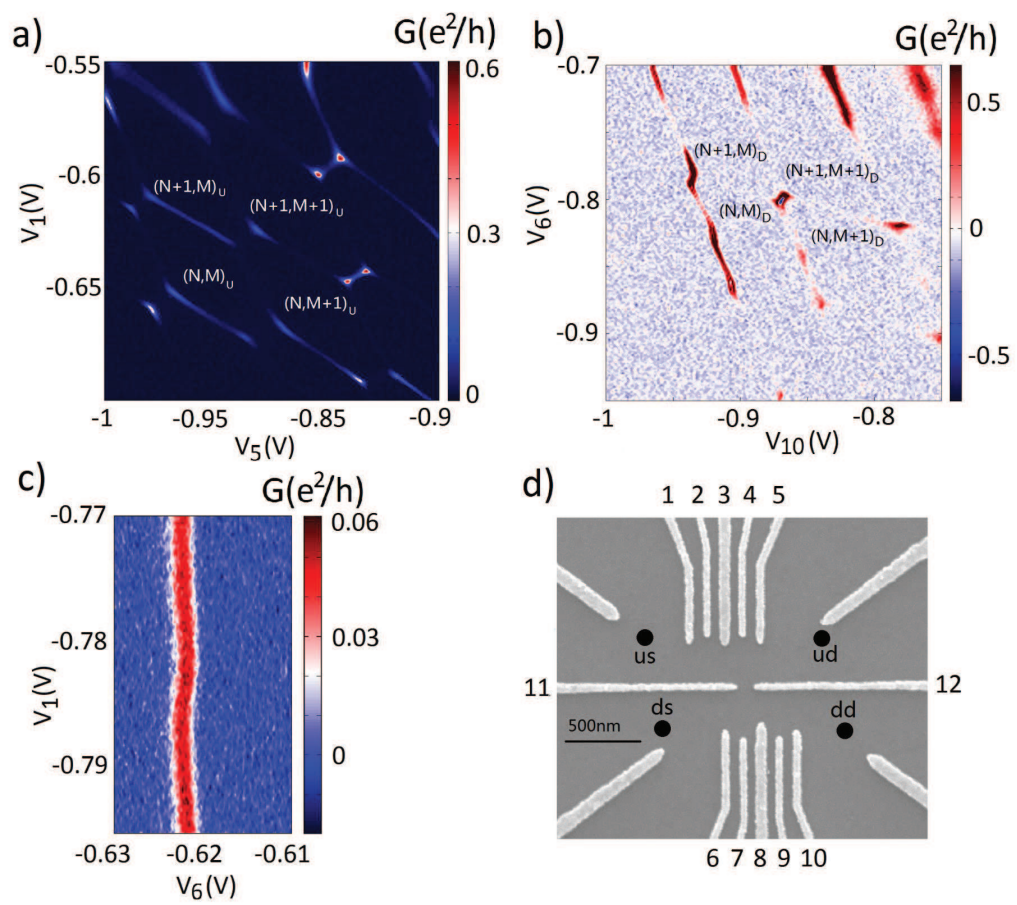


Figure 1 LY14410 22APR2015

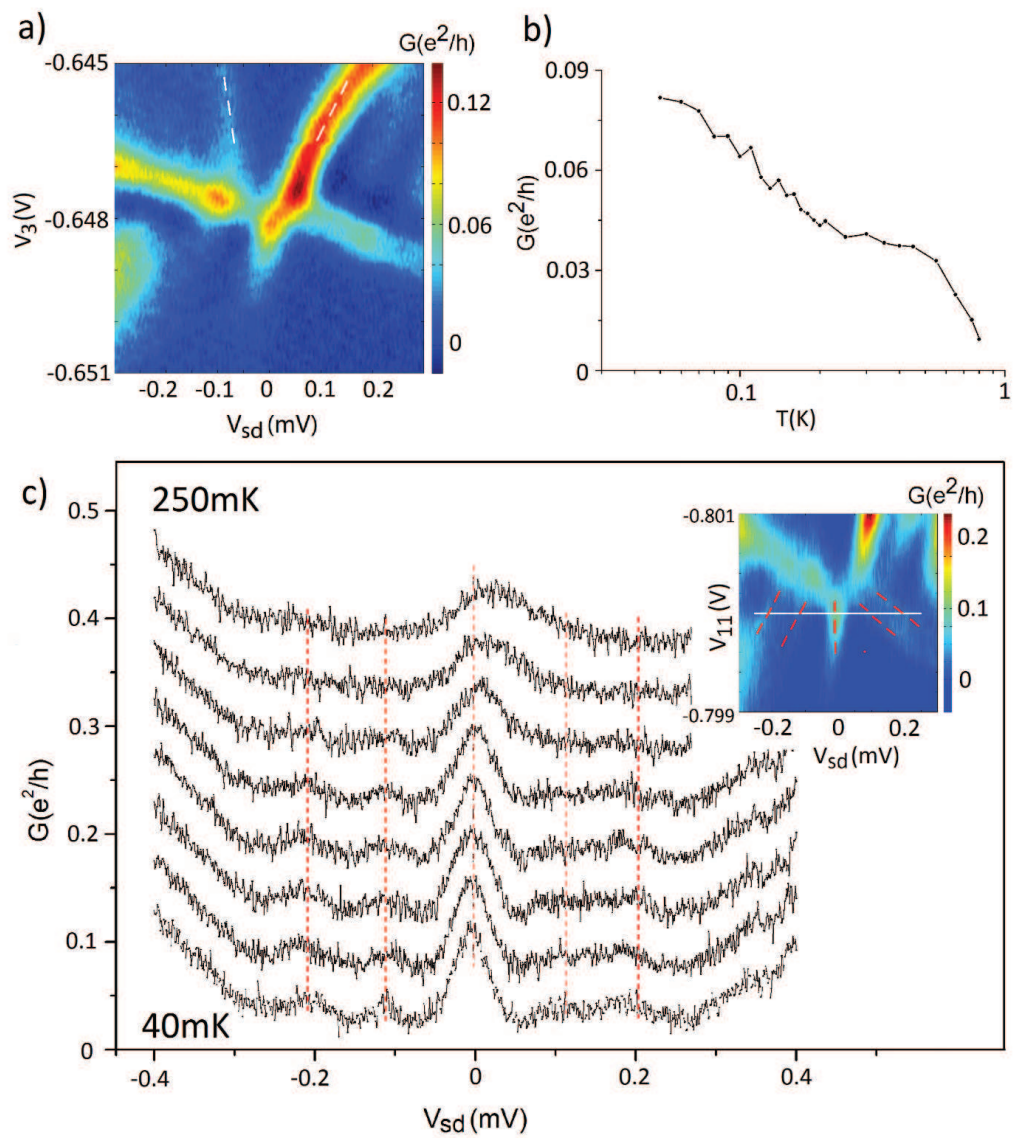


Figure 2

LY14410

22APR2015

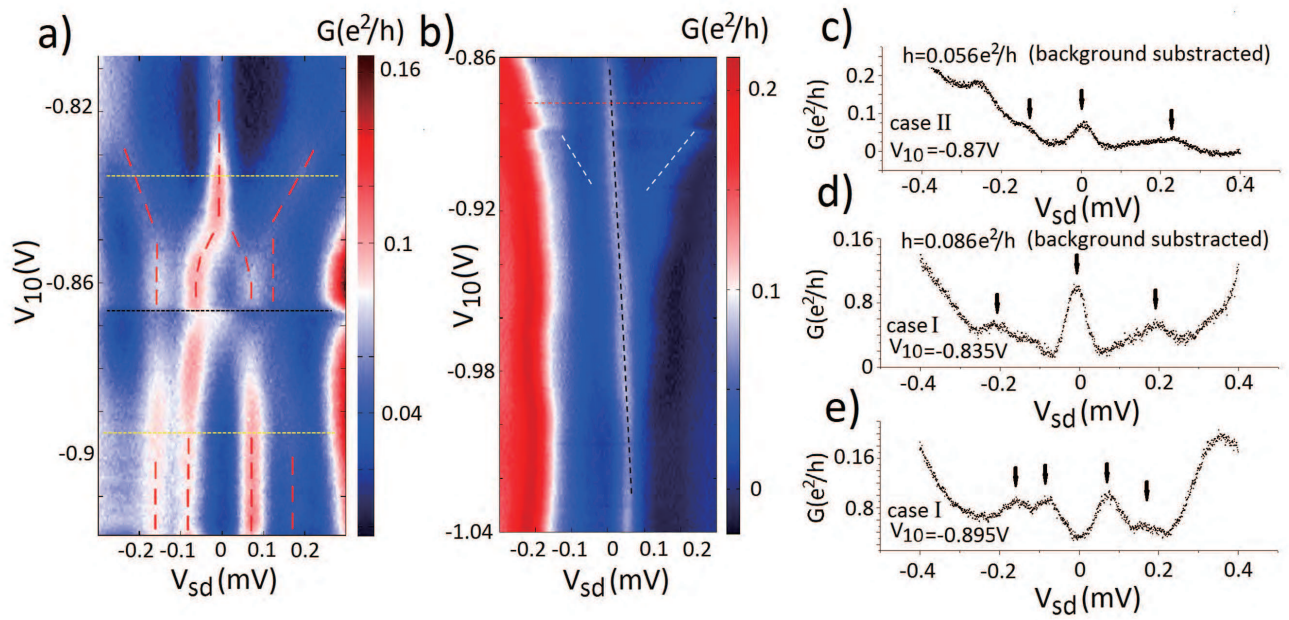


Figure 3

LY14410

22APR2015

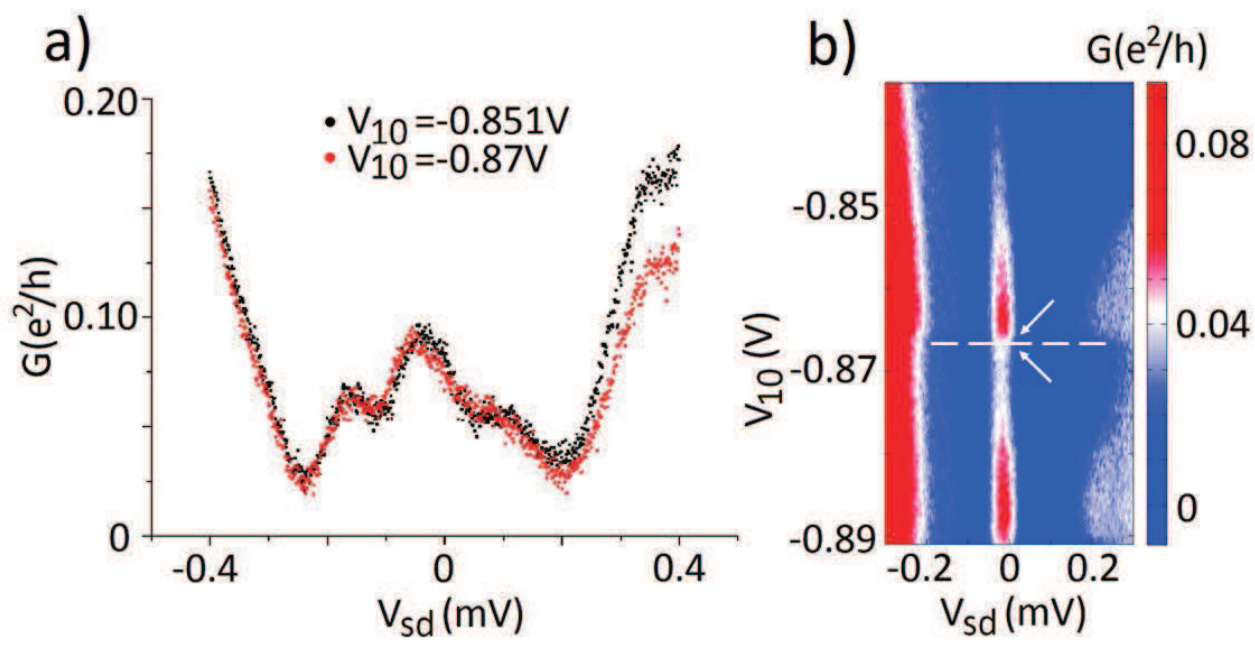


Figure 4 LY14410 22APR2015